Coherence in Large-Scale Networks: Dimension-Dependent Limitations of Local Feedback

Bassam Bamieh, *Fellow, IEEE,* Mihailo R. Jovanović, *Member, IEEE,* Partha Mitra, *Senior Member, IEEE,* and Stacy Patterson, *Associate Member, IEEE*

Abstract—We consider distributed consensus and vehicular formation control problems. Specifically we address the question of whether local feedback is sufficient to maintain coherence in large-scale networks subject to stochastic disturbances. We define macroscopic performance measures which are global quantities that capture the notion of coherence; a notion of global order that quantifies how closely the formation resembles a solid object. We consider how these measures scale asymptotically with network size in the topologies of regular lattices in 1, 2, and higher dimensions, with vehicular platoons corresponding to the 1-D case. A common phenomenon appears where a higher spatial dimension implies a more favorable scaling of coherence measures, with a dimensions of 3 being necessary to achieve coherence in consensus and vehicular formations under certain conditions. In particular, we show that it is impossible to have large coherent 1-D vehicular platoons with only local feedback. We analyze these effects in terms of the underlying energetic modes of motion, showing that they take the form of large temporal and spatial scales resulting in an accordion-like motion of formations. A conclusion can be drawn that in low spatial dimensions, local feedback is unable to regulate large-scale disturbances, but it can in higher spatial dimensions. This phenomenon is distinct from, and unrelated to string instability issues which are commonly encountered in control problems for automated highways.

Index Terms—Vehicular formation.

I. INTRODUCTION

THE control problem for strings of vehicles (the so-called platooning problem) has been extensively studied in the last two decades, with original problem formulations and studies dating back to the 60's [1]–[5]. These problems are also intimately related to more recent formation flying and formation control problems [6]. It has long been observed in platooning problems that to achieve reasonable performance, certain global

information such as leader's position or state need to be broadcast to the entire formation. A precise analysis of the limits of performance associated with localized versus global control strategies does not appear to exist in the formation control literature. In this paper we study the platooning problem as the 1-D version of a more general vehicular formations control problem on regular lattices in arbitrary spatial dimensions. For such problems, we investigate the limits of performance of any local feedback law that is globally stabilizing. In particular, we propose and study measures of the coherence of the formation. These are measures that capture the notion of how well the formation resembles a rigid lattice or a solid object.

The coherence of a formation is a different concept from, and often unrelated to, string instability. In the platooning case (i.e., 1-D formations), which turns out to be most problematic, a localized feedback control law may posses string stability in the sense that the effects of any injected disturbance do not grow with spatial location. However, as we show in this paper, it is impossible to achieve a large coherent formation with only localized feedback if all vehicles are subject to any amount of distributed stochastic disturbances. The net effect is that with the best localized feedback, a 1-D formation will appear to behave well on a "microscopic" scale in the sense that distances between neighboring vehicles will be well regulated. However, if a large formation is observed in its entirety, it will appear to have temporally slow, long spatial wavelength modes that are unregulated, resembling an "accordion" type of motion. This is not a safety issue, since the formation is microscopically well regulated, but it might effect throughput performance in a platooning arrangement since throughput does depend on the coherence or rigidity of the formation.

The phenomenon that we discuss occurs in both consensus algorithms and vehicular formation problems. We therefore treat both as instances of networked dynamical systems with first order and second order local dynamics respectively. Both problems are set up in the d-dimensional torus $\mathbb{Z}_N^d$. We begin in Section II with problem formulations of the consensus type and vehicular formations, where we view the former as a first order dynamics version of the latter. In Section III, we define macroscopic and microscopic measures of performance in terms of variances of various quantities across the network. We argue that the macroscopic measures capture the notion of coherence. We also present compact formulae for calculating those measures as H^2 norms of systems with suitably defined output signals. These norms are calculated using traces of system Grammians, which in turn are related to sums involving eigenvalues of the underlying system and feedback gains matrices. Since the network topologies we consider are built over Tori networks, these

system matrices are multidimensional circulant operators, and their eigenvalues are calculated as the values of the Fourier symbols of the underlying feedback operators, thus allowing for a rather direct relation between the structure of the feedback gains and the system's norms. Much of the remainder of the paper is devoted to establishing asymptotic (in network size) bounds for these performance measures for each underlying spatial dimension. Section IV establishes upper bounds of standard algorithms, while Section V is devoted to establishing lower bounds for *any* algorithm that satisfies a certain number of structural assumptions including the locality of feedback and boundedness of control effort. This shows that asymptotic limits of performance are determined by the network structure rather than the selection of parameters of the feedback algorithm. We pay particular attention to the role of control effort as our lower bounds are established for control laws that have bounded control effort in a stochastic sense. Some numerical examples illustrating the lack-of-coherence phenomenon are presented in Section VI, as well as an illustration of how it is distinct from string instability. The interested reader may initially skim this section which numerically illustrates the basic phenomenon we study analytically in the remainder of the paper. We end in Section VII with a discussion of related work in which various versions of this phenomenon were observed, as well as a discussion of some open questions.

Notation and Preliminaries: The networks we consider are built over the d-dimensional Torus $\mathbb{Z}_N^d$. The 1-D Torus $\mathbb{Z}_N$ is simply the set of integers $\{0, 1, \ldots, N-1\}$ with addition *modulo* N $(\mathrm{mod}N)$, and $\mathbb{Z}_N^d$ is the direct product of d copies of $\mathbb{Z}_N$. Functions defined on $\mathbb{Z}_N^d$ are called *arrays*, and we use multi-index notation for them, as in $a_k = a_{(k_1,\ldots,k_d)}$ to denote individual entries of an array. Indices are added in the $\mathbb{Z}_N^d$ arithmetic as follows:

$$(r_1, \ldots, r_d) = (k_1, \ldots, k_d) + (l_1, \ldots, l_d)$$
$$\Updownarrow$$
$$r_i = (k_i + l_i)_N, \quad i = 1, \ldots, d$$

where $()_N$ is the operation $\mathrm{mod}N$. The set $\mathbb{Z}_N^d$ and the corresponding addition operation can be visualized as a "circulant" graph in d-dimensional space with edge nodes connected to nodes on corresponding opposite edge of the graph.

The multidimensional Discrete Fourier Transform is used throughout. All states are multidimensional arrays which we define as real or complex vector-valued functions on the Torus $\mathbb{Z}_N^d$. The Fourier transform (Discrete Fourier Transform) of an array a is denoted with $\hat{a}$. We refer to indices of spatial Fourier transforms as *wavenumbers*. Generally, we use k and l for spatial indices and n and m for wavenumbers. For example, an array $a_{(k_1,\ldots,k_d)}$ has $(k_1, \ldots, k_d)$ as the spatial index, while its Fourier transform $\hat{a}_{(n_1,\ldots,n_d)}$ has the index $(n_1, \ldots, n_d)$ as the wavenumber. The wavenumber is simply a spatial frequency variable. Some elementary properties of this Fourier transform are summarized in Appendix A.

Convolution operators arise naturally over $\mathbb{Z}_N^d$. Let a be any array of numbers (or matrices) over $\mathbb{Z}_N^d$, that is $a : \mathbb{Z}_N^d \to \mathbb{C}$ (or $\mathbb{C}^{n \times n}$). Then the operator T_a of multi-dimensional circular convolution with the array a is defined as follows:

$$g = T_a f = a \star f$$
$$\Updownarrow$$
$$g_{(k_1,\ldots,k_d)} = \sum_{(l_1,\ldots,l_d) \in \mathbb{Z}_N^d} a_{(k_1,\ldots,k_d)-(l_1,\ldots,l_d)} f_{(l_1,\ldots,l_d)}.$$

Note that f and g may be scalar or vector-valued (depending on whether a is scalar or matrix-valued respectively), and that the arithmetic for $(k_1, \ldots, k_d) - (l_1, \ldots, l_d)$ is done in $\mathbb{Z}_N^d$, i.e. arithmetic $\mathrm{mod}N$ in each index as described above.

It is important to distinguish between an array a and the corresponding linear operator T_a. The Fourier transform $\hat{a}$ of the array a is called the *Fourier symbol* of the operator T_a. It is a standard fact that the eigenvalues of the operator T_a are exactly the values of the Fourier transform $\hat{a}$, i.e. the values of its Fourier symbol. When a is matrix valued, then the eignvalues of T_a are the union of all eigenvalues of $\hat{a}_{(n_1,\ldots,n_d)}$ as the wavenumber $(n_1, \ldots, n_d)$ runs through $\mathbb{Z}_N^d$, i.e.

$$\sigma(T_a) = \bigcup_{(n_1,\ldots,n_d) \in \mathbb{Z}_N^d} \sigma\left(\hat{a}_{(n_1,\ldots,n_d)}\right)$$

where $\sigma(.)$ refers to the spectrum of a matrix or operator (all finite-dimensional in our case).

In this paper, we use the term *dimension* to refer exclusively to the spatial dimension of underlying networks. To avoid confusion with the notion of state dimension, we refer to the dimension of the state space of any dynamical system as the *order* of that dynamical system.

The vector dimension of signals is mostly suppressed to keep the notation from being cumbersome. For example, the state of node $(k_1, \ldots, k_d)$ in the d-dimensional Torus is written as

$$x_{(k_1,\ldots,k_d)}(t).$$

It is a scalar-valued signal for consensus problems, and vector-valued (in $\mathbb{R}^d$) signal for vehicular formation problems.

We use M^T to denote the transpose of a matrix M, and M^* to denote the complex-conjugate transpose of a matrix M or the adjoint of an operator M. Although all operators in this paper are finite dimensional, we sometimes refer to them as operators rather than matrices since we often avoid writing the cumbersome explicit matrix representations (such as in the case of multidimensional convolution operators).

II. PROBLEM FORMULATION

We formulate two types of problems, consensus and vehicular formations. The mathematical setting is analogous in both problems, with the main difference being that vehicular models have two states (position and velocity) locally at each site in contrast to a scalar local state in consensus problem. This difference leads to more severe asymptotic scalings in vehicular formations as will be shown in the sequel.

A. Consensus With Random Insertions/Deletions

We begin by formulating a continuous-time version of the consensus algorithm with additive stochastic disturbances in the dynamics [7], [8]. As opposed to standard consensus algorithms without additive disturbances, nodes do not achieve equilibrium asymptotically but fluctuate around the equilibrium, and the variance of this fluctuation is a measure of how well approximate consensus is achieved. This formulation can be used to model scenarios such as load balancing over a distributed file system, where the additive noise represents file insertion and deletion, parallel processing systems where the noise processes model job creation and completion, or flocking problems in the presence of random forcing disturbances.

We consider a consensus algorithm over undirected tori, $\mathbb{Z}_N^d$, where the derivative of the scalar state at each node is determined as a weighted average of the differences between that node and all its $2d$ neighbors. One possible such algorithm is given by

$$
\begin{aligned}
\dot{x}_k =& \beta\big[(x_{(k_1-1,\dots,k_d)} - x_k) + \cdots + (x_{(k_1,\dots,k_d+1)} - x_k)\big] + w_k, \\
=& (-2d\beta)x_k + \beta\big[x_{(k_1-1,\dots,k_d)} + x_{(k_1+1,\dots,k_d)} + \cdots \\
& \qquad + x_{(k_1,\dots,k_d-1)} + x_{(k_1,\dots,k_d+1)}\big] + w_k \quad (1)
\end{aligned}
$$

where we have used equal weights $\beta > 0$ for all the differences. The process disturbance w is a mutually uncorrelated white stochastic process. We call this the *standard consensus algorithm* in this paper since it is essentially the same as other well-studied consensus algorithms [9]–[13].

The sum in the equation above can be written as a multidimensional convolution by defining the array

$$
O_{(k_1,\dots,k_d)} = \begin{cases} -2d\beta & k_1 = \cdots = k_d = 0, \\ \beta & k_i = \pm 1, \text{ and } k_j = 0 \text{ for } i \neq j, \\ 0 & \text{otherwise.} \end{cases}
$$
$$(2)$$

The system (1) can then be written as

$$
\dot{x} = O \star x + w \quad (3)
$$

where $\star$ is circular convolution in $\mathbb{Z}_N^d$.

We recall that we use the operator notation $T_a x := a \star x$ to indicate the circulant operator of convolution with any array a. With this notation, a general spatially invariant consensus algorithm can be written abstractly as

$$
\dot{x} = T_a x + w \quad (4)
$$

for any array a defined over $\mathbb{Z}_N^d$. Such algorithms can be regarded as a combination of open loop dynamics

$$
\dot{x}_k = u_k + w_k, \quad k \in \mathbb{Z}_N^d
$$

with the feedback "control" $u = T_a x$, where the feedback operator array is to be suitably designed. With this point of view, consensus algorithms can be thought of as first order dynamics versions of vehicular formation problems that we introduce next.

B. Vehicular Formations

Consider N^d identical vehicles arranged in a d-dimensional torus, $\mathbb{Z}_N^d$, with the double integrator dynamics

$$
\ddot{x}_{(k_1,\dots,k_d)} = u_{(k_1,\dots,k_d)} + w_{(k_1,\dots,k_d)} \quad (5)
$$

where $(k_1,\dots,k_d)$ is a multi-index with each $k_i \in \mathbb{Z}_N$, u is the control input and w is a mutually uncorrelated white stochastic process which can be considered to model random forcing. In the sequel, we will also consider the consequences of the presence of viscous friction terms in models of the form

$$
\ddot{x}_{(k_1,\dots,k_d)} = -\mu\dot{x}_{(k_1,\dots,k_d)} + u_{(k_1,\dots,k_d)} + w_{(k_1,\dots,k_d)} \quad (6)
$$

where $\mu > 0$ is the linearized drag coefficient per unit mass.

Each position vector x_k is a d-dimensional vector with components $x_k = [x_k^1 \cdots x_k^d]^T$. The objective is to have the kth vehicle in the formation follow the desired trajectory $\bar{x}_k$:

$$
\bar{x}_k := \bar{v}t + k\Delta \Leftrightarrow \begin{bmatrix} \bar{x}_k^1 \\ \vdots \\ \bar{x}_k^d \end{bmatrix} := \begin{bmatrix} \bar{v}^1 \\ \vdots \\ \bar{v}^d \end{bmatrix} t + \begin{bmatrix} k_1 \\ \vdots \\ k_d \end{bmatrix} \Delta
$$

which means that all vehicles are to move with constant heading velocity $\bar{v}$ while maintaining their respective position in a $\mathbb{Z}_N^d$ grid with spacing of Δ in each dimension. The situation of different spacings in different directions can be similarly represented, but is not considered for notational simplicity.

The deviations from desired trajectory are defined as

$$
\tilde{x}_k := x_k - \bar{x}_k, \tilde{v}_k := \dot{x}_k - \bar{v}.
$$

We assume the control input to be full state feedback and linear in the variables $\tilde{x}$ and $\tilde{v}$ (therefore affine linear in x and v), i.e. $u = G\tilde{x} + F\tilde{v}$, where G and F are the linear feedback operators. The equations of motion for the controlled system are thus

$$
\frac{d}{dt}\begin{bmatrix} \tilde{x} \\ \tilde{v} \end{bmatrix} = \begin{bmatrix} 0 & I \\ G & F \end{bmatrix}\begin{bmatrix} \tilde{x} \\ \tilde{v} \end{bmatrix} + \begin{bmatrix} 0 \\ I \end{bmatrix}w. \quad (7)
$$

We note that the above equations are written in operator form, i.e. by suppressing the spatial index of all the variables.

Example: The operators G and F will have some very special structure depending on assumptions of the type of feedback and measurements available. Consider for example a feedback control of the kth vehicle (in a 1-D formation) of the following form:

$$
\begin{aligned}
u_k = g_+(x_{k+1} - x_k - \Delta) + g_-(x_{k-1} - x_k - \Delta) + f_+(v_{k+1} - v_k) \\
+ f_-(v_{k-1} - v_k) + g_o(x_k - \bar{x}_k) + f_o(v_k - \bar{v})
\end{aligned}
$$

where the g's and f's are design constants. The first two lines represent look-ahead and look-behind position and velocity error feedbacks respectively. We refer to such terms as *relative feedback* since they *only* involve measurements of differences. On the other hand, terms in the last line require knowledge of positions and velocities in an absolute coordinate system (a grid moving at constant velocity), and we thus refer to such terms as *absolute feedback*. For later reference, it is instructive to write the feedback in the above example in terms of the state variables $\tilde{x}$ and $\tilde{v}$ as

$$
\begin{aligned}
u_k = g_+(\tilde{x}_{k+1} - \tilde{x}_k) + g_-(\tilde{x}_{k-1} - \tilde{x}_k) + f_+(\tilde{v}_{k+1} - \tilde{v}_k) \\
+ f_-(\tilde{v}_{k-1} - \tilde{v}_k) + g_o\tilde{x}_k + f_o\tilde{v}_k. \quad (8)
\end{aligned}
$$

C. Structural Assumptions

We now list the various assumptions that can be imposed on system operators and on the control feedbacks G and F. These are structural restrictions representing the structure of open loop dynamics and measurements, and the type of feedback control available respectively.

(A1) Spatial Invariance. All operators are spatially invariant with respect to $\mathbb{Z}_N^d$. This implies that they are convolution operators. For instance, the operation Gx can be

written as the convolution (over $\mathbb{Z}_N^d$) of the array x with an array $\{G_{(k_1,\ldots,k_d)}\}$

$$(Gx)_k = \sum_{l \in \mathbb{Z}_N^d} G_{k-l} x_l \qquad (9)$$

where the arithmetic for $k-l$ is done in $\mathbb{Z}_N^d$. For each k, the array element G_k is a $d \times d$ matrix (G is then an $N^d \times N^d$ operator). Note that in the absence of spatial invariance, each term of the sum in (9) would need to be written as $G_{k,l} x_l$. That is, one would require a two-indexed array of matrices $G_{k,l}$ rather than a single-indexed array.

In the example above of a 1-D circular formation, the array elements for position feedback are given by $\{(g_o - g_+ - g_-), g_+, 0, \ldots, 0, g_-\}$.

(A2) Relative vs. Absolute Feedback. We use the term Relative Feedback when given feedback involves only differences between quantities. For example, in position feedback, this implies that for each term of the form $\alpha x_{(k_1,\ldots,k_d)}$ in the convolution, another term of the form $-\alpha x_{(l_1,\ldots,l_d)}$ occurs for some other multi-index l. This implies that the array G has the property

$$\sum_{k \in \mathbb{Z}_N^d} G_k = 0. \qquad (10)$$

We use the term Absolute Feedback when given operator does not satisfy this assumption.

Note that in the example above, relative position feedback corresponds to $g_o = 0$, and in this case, condition (10) is satisfied.

(A3) Locality. The feedbacks use only local information from a neighborhood of width $2q$, where q is independent of N. Specifically

$$G_{(k_1,\ldots,k_d)} = 0, \quad \text{if} \quad k_i > q, \quad \text{and} \quad k_i < N - q$$
$$\text{for any} \quad i \in \{1,\ldots,d\}. \quad (11)$$

The same condition holds for F.

(A4) Reflection Symmetry. The interactions between vehicles have mirror symmetry. This has the consequence that the arrays representing G and F have even symmetry, e.g. for each nonzero term like $\alpha G_{(k_1,\ldots,k_d)}$ in the array there is a corresponding term $\alpha G_{(-k_1,\ldots,-k_d)}$. This in particular implies that the Fourier symbols of G and F are real valued. In the example above, this condition gives $g_+ = g_-$ and $f_+ = f_-$.

(A5) Coordinate Decoupling. For $d \geq 2$, feedback control of thrust in each coordinate direction depends only on measurements of position and velocity error vector components in that coordinate. This is equivalent to imposing that each array element G_k and F_k are $d \times d$ diagonal matrices. For further simplicity we assume those diagonal elements to be equal, i.e.

$$G_k = \text{diag}\{g_k, \ldots, g_k\}, \quad F_k = \text{diag}\{f_k, \ldots, f_k\}. \quad (12)$$

This in effect renders the matrix-vector convolution in (9) into d decoupled scalar convolutions.

Assumptions **(A1)** through **(A3)** appear to be important for subsequent developments, while assumptions **(A4)** and **(A5)** are made to simplify calculations.

III. PERFORMANCE MEASURES

We will consider how various performance measures scale with system size for the consensus and vehicle formations problems. Some of these measures can be quantified as steady state variances of outputs of linear systems driven by stochastic inputs, so we consider some generalities first. Consider a general linear system driven by zero mean white noise with unit covariance

$$\dot{x} = Ax + Bw,$$
$$y = Hx.$$

Since we are interested in cases where A is not necessarily Hurwitz (typically due to a single unstable mode at the origin representing motion of the mean), the state x may not have finite steady state variances. However, in all cases we consider here the outputs y do have finite variances, i.e. the unstable modes of A are not observable from y. In such cases, the output does have a finite steady state variance, which is quantified by the square of the H^2 norm of the system from w to y

$$V := \sum_{k \in \mathbb{Z}_N^d} \lim_{t \to \infty} E\{y_k^*(t) y_k(t)\} \qquad (13)$$

where the index k ranges over all "sites" in the lattice $\mathbb{Z}_N^d$.

We are interested in spatially invariant problems over discrete Tori. This type of invariance implies that the variances of all outputs are equal, i.e. $E\{y_k^* y_k\}$ is independent of k. Thus, if the output variance at a given site is to be computed, it is simply the total H^2 norm divided by the system size

$$E\{y_k^* y_k\} = \frac{1}{M} \sum_{l \in \mathbb{Z}_N^d} E\{y_l^* y_l\} = \frac{V}{M} \qquad (14)$$

where M is the size of the system ($M = N^d$ for d-dimensional Tori). We refer to quantities like (14) as *individual output variances*.

Next, we define several different performance measures and give the corresponding output operators for each measure for both the consensus and vehicular formation problems. In the vehicular formation problem, we assume for simplicity that the output involves positions only, and thus the output equation has the form

$$y = \begin{bmatrix} C & 0 \end{bmatrix} \begin{bmatrix} \tilde{x} \\ \tilde{v} \end{bmatrix}$$

i.e. $H = \begin{bmatrix} C & 0 \end{bmatrix}$, where C is a circulant operator. A consensus problem with the same performance measure has a corresponding output equation of the form (with the same C operator)

$$y = Cx.$$

Performance Measures: We now list the three different performance measures we consider.

(P1) Local error. This is a measure of the difference between neighboring nodes or vehicles. For the consensus problem, the kth output (in the case of one dimension) is defined by

$$y_k := x_k - x_{k-1}.$$

For the case of vehicular formations, local error is the difference of neighboring vehicles positions from desired spacing, which can equivalently be written as

$$y_k := \tilde{x}_k - \tilde{x}_{k-1}.$$

The output operator is then given by $C := (I - D)$, where D is the right shift operator, $(Dx)_k := x_{k-1}$.

In the case of d dimensions, we define a vector output that contains as components the local error in each respective dimension, i.e.

$$C := \frac{1}{\sqrt{2d}}[I - D^1 \quad \cdots \quad I - D^d]^T \qquad (15)$$

where D^r is the right shift along the rth dimension, i.e. $(D^r x)_{(k_1,\ldots,k_r,\ldots,k_d)} := x_{(k_1,\ldots,k_r-1,\ldots,k_d)}$, and $1/\sqrt{2d}$ is a convenient normalization factor. This operator is closely related to the standard consensus operator O in (2) by the following easily established identity:

$$C^*C = \frac{-1}{2d\beta}O. \qquad (16)$$

(P2) Long range deviation (Disorder). In the consensus problem, this corresponds to measuring the disagreement between the two furthest nodes in the network graph. Assume for simplicity that N is even and we are in dimension 1. Then, the most distant node from node k is $N/2$ hops away, and we define

$$y_k := x_k - x_{k+\frac{N}{2}}.$$

In the vehicular formation problem, long range deviation corresponds to measuring the deviation of the distance between the two most distant vehicles from what it should be. The most distant vehicle to the kth one is the vehicle indexed by $k + (N/2)$. The desired distance between them is $\Delta(N/2)$, and the deviation from this distance is

$$y_k := x_k - x_{k+\frac{N}{2}} - \Delta\frac{N}{2} = \tilde{x}_k - \tilde{x}_{k+\frac{N}{2}}. \qquad (17)$$

We consider the variance of this quantity to be a measure of disorder, reflecting the lack of "end-to-end rigidity" in the vehicle formation.

Generalizing this measure to d dimensions yields an output operator of the form

$$C := T_{\left(\boldsymbol{\delta}^0 - \boldsymbol{\delta}^{(\frac{N}{2},\ldots,\frac{N}{2})}\right)} \qquad (18)$$

i.e. the operator of convolution with the array[1] $\boldsymbol{\delta}^0 - \boldsymbol{\delta}^{(N/2,\ldots,N/2)}$.

---

[1] By a slight abuse of notation, we define the shifted Kronecker delta $\boldsymbol{\delta}^l_k := \delta_{k-l}$, where $\delta_k = 1$ for $k = 0$, and zero otherwise, is the standard Kronecker delta. With this notation, $\boldsymbol{\delta}^0$ is also the standard Kronecker delta.

(P3) Deviation from average. For the consensus problem, this quantity measures the deviation of each state from the average of all states

$$y_k := x_k - \frac{1}{M}\sum_{l\in\mathbb{Z}_N^d} x_l. \qquad (19)$$

In operator form we have $y = (I - T_{\bar{1}})x$, where $\bar{1}$ is the array of all elements equal to $1/M$.

In vehicular formations, this measure can be interpreted as the deviation of each vehicle's position error from the average of the overall position error $y = (I - T_{\bar{1}})\tilde{x}$.

We note that performance measures **(P1)** through **(P3)** are such that C can be represented as a convolution with an array $\{C_k\}$ which has the property $\sum_{k\in\mathbb{Z}_N^d} C_k = 0$. This condition causes the mean mode at zero to be unobservable, and thus guarantees that all outputs defined above have finite variances.

We refer to the performance measure **(P1)** as a *microscopic error* since it involves quantities local to any given site. This is in contrast to the measures **(P2)** and **(P3)** which involve quantities that are far apart in the network, and we thus refer to these as *macroscopic errors*. We consider the macroscopic errors as measures of disorder or equivalently, lack of coherence. As we will show in the sequel, both macroscopic measures scale similarly asymptotically with system size, which justifies using either of them as a measure of disorder.

Formulae for Variances: Since we consider spatially invariant systems and in particular systems on the discrete Tori $\mathbb{Z}_N^d$, it is possible to derive formulae for the above defined measures in terms of the Fourier symbols of the operators K, F and C. Recall the state space formula for the H^2 norm V defined in (13)

$$V = \text{tr}\left(\int_0^\infty B^* e^{A^*t} H^* H e^{At} B \, dt\right).$$

When A, B and H are circulant operators, traces can be rewritten in terms of their respective Fourier symbols [see (47)] as

$$V = \text{tr}\left(\sum_n \int_0^\infty \hat{B}_n^* e^{\hat{A}_n^*t} \hat{H}_n^* \hat{H}_n e^{\hat{A}_n t} \hat{B}_n \, dt\right) \qquad (20)$$

$$= \sum_n \text{tr}\left(\hat{B}_n^* \hat{P}_n \hat{B}_n\right) \qquad (21)$$

where the individual integrals are defined as

$$\hat{P}_n := \int_0^\infty e^{\hat{A}_n^*t} \hat{H}_n^* \hat{H}_n e^{\hat{A}_n t} \, dt. \qquad (22)$$

If $\hat{A}_n$ is Hurwitz, then $\hat{P}_n$ can be obtained by solving the Lyapunov equation

$$\hat{A}_n^* \hat{P}_n + \hat{P}_n \hat{A}_n = -\hat{H}_n^* \hat{H}_n. \qquad (23)$$

For wavenumbers n for which $\hat{A}_n$ is not Hurwitz, $\hat{P}_n$ is still finite if the non-Hurwitz modes of $\hat{A}_n$ are not observable from $\hat{H}_n$. In this case we can analyze the integral in (22) on a case by case basis.

TABLE I
SUMMERY OF ASYMPTOTIC SCALINGS OF UPPER BOUNDS IN TERMS OF THE THE TOTAL NETWORK SIZE M AND THE SPATIAL DIMENSIONS d. PERFORMANCE MEASURES ARE CLASSIFIED AS EITHER MICROSCOPIC (LOCAL ERROR), OR MACROSCOPIC (DEVIATION FROM AVERAGE OR LONG RANGE DEVIATION). THERE ARE FOUR POSSIBLE FEEDBACK STRATEGIES IN VEHICULAR FORMATIONS DEPENDING ON WHICH COMBINATION OF RELATIVE OR ABSOLUTE POSITION OR VELOCITY ERROR FEEDBACK IS USED. QUANTITIES LISTED ARE UP TO A MULTIPLICATIVE FACTOR THAT IS INDEPENDENT OF M OR ALGORITHM PARAMETER β

	Microscopic	Macroscopic
Consensus	$1/\beta$	$\frac{1}{\beta}\begin{cases} M & d=1 \\ \log(M) & d=2 \\ 1 & d\geq 3 \end{cases}$
Vehicular Formations Feedback type: abs. pos. & abs. vel.	$1/\beta$	1
Vehicular Formations Feedback type: rel. pos. & abs. vel. or abs. pos. & rel. vel.	$1/\beta$	$\frac{1}{\beta}\begin{cases} M & d=1 \\ \log(M) & d=2 \\ 1 & d\geq 3 \end{cases}$
Vehicular Formations Feedback type: rel. pos. & rel. vel.	$\frac{1}{\beta^2}\begin{cases} M & d=1 \\ \log(M) & d=2 \\ 1 & d\geq 3 \end{cases}$	$\frac{1}{\beta^2}\begin{cases} M^3 & d=1 \\ M & d=2 \\ M^{1/3} & d=3 \\ \log(M) & d=4 \\ 1 & d\geq 5 \end{cases}$

The Lyapunov equations are easy to solve in the Fourier domain. Equation (23) is a scalar equation in the Consensus case and a $2d \times 2d$ matrix equation in the Vehicular case.[2] The two respective calculations are summarized in the next lemma. The proof is given in the Appendix.

Lemma 3.1: The output variances (13) for the consensus and vehicular problems satisfying assumptions **(A1)**–**(A5)** are given

$$V_c = -\frac{1}{2} \sum_{n\neq 0, n\in\mathbb{Z}_N^d} \frac{|\hat{c}_n|^2}{\Re(\hat{a}_n)} \tag{24}$$

$$V_v = \frac{d}{2} \sum_{n\neq 0, n\in\mathbb{Z}_N^d} \frac{|\hat{c}_n|^2}{\hat{g}_n \hat{f}_n} \tag{25}$$

where $\Re(\hat{a}_n)$ is the real part of $\hat{a}_n$, $\hat{c}$ is the Fourier symbol of the output operator corresponding to the performance index under consideration, and $\hat{a}$, $\hat{g}$ and $\hat{f}$ are the Fourier symbols of the consensus operator (4), and the position and velocity feedback operators (12) respectively.

These expressions can then be worked out for the variety of output operators C representing the different performance measures defined earlier. The next result presents a summary of those calculations for the six different cases.

Corollary 3.2: The following are performance measures **(P1)**, **(P2)** and **(P3)** expressed in terms of the Fourier symbols $\hat{g}$, $\hat{f}$ and $\hat{a}$, of the operators G, F, and T_a defining vehicular formations and consensus algorithms which satisfy assumptions **(A1)**–**(A5)**. The array O is that of the standard consensus algorithm (2).

1) *Consensus*
   a) Local Error:

$$V_c^{loc} = \frac{1}{4d}\frac{1}{\beta} \sum_{n\neq 0, n\in\mathbb{Z}_N^d} \frac{\hat{O}_n}{\Re(\hat{a}_n)}. \tag{26}$$

   b) Long Range Deviation:

$$V_c^{lrd} = -2 \sum_{n_1+\cdots+n_d \text{odd}, n\in\mathbb{Z}_N^d} \frac{1}{\Re(\hat{a}_n)}. \tag{27}$$

   c) Deviation from Average:

$$V_c^{dav} = -\frac{1}{2} \sum_{n\neq 0, n\in\mathbb{Z}_N^d} \frac{1}{\Re(\hat{a}_n)}. \tag{28}$$

2) *Vehicular Formations*
   a) Local Error:

$$V_v^{loc} = -\frac{1}{4}\frac{1}{\beta} \sum_{n\neq 0, n\in\mathbb{Z}_N^d} \frac{\hat{O}_n}{\hat{g}_n \hat{f}_n}. \tag{29}$$

   b) Long Range Deviation:

$$V_v^{lrd} = 2d \sum_{n_1+\cdots+n_d \text{odd}, n\in\mathbb{Z}_N^d} \frac{1}{\hat{g}_n \hat{f}_n}. \tag{30}$$

   c) Deviation from Average:

$$V_v^{dav} = \frac{d}{2} \sum_{n\neq 0, n\in\mathbb{Z}_N^d} \frac{1}{\hat{g}_n \hat{f}_n}. \tag{31}$$

IV. UPPER BOUNDS USING STANDARD ALGORITHMS

In this section we derive asymptotic upper bounds for all three performance measures of both the consensus and vehicular problems. These bounds are derived by exhibiting simple feedback laws similar to the one in the standard consensus algorithm (2). In the case of vehicular formations, we make a distinction between the cases of relative versus absolute position and velocity feedbacks, and derive bounds for all four possible combinations of such feedbacks.

The behavior of the asymptotic bounds has an important dependence on the underlying spatial dimension d. For the purpose of cross comparison, all of the upper bounds derived in this section are summarized in Table I.

For later reference, we note that the Fourier transform of the array O in (2) is a quantity that occurs often, and calculated as

$$\hat{O}h_n = -2d\beta + \sum_{r=1}^{d} \left(\beta e^{-i\frac{2\pi}{N}n_r} + \beta e^{i\frac{2\pi}{N}n_r} \right)$$

$$= -2\beta \sum_{r=1}^{d} \left(1 - \cos\left(\frac{2\pi}{N}n_r\right) \right). \tag{32}$$

A. Upper Bounds in the Consensus Case

We consider the standard consensus algorithm (1). In this case the array a is exactly O, and thus expression (26) for the local error immediately simplifies to

$$V_c^{loc} = \frac{1}{4d\beta} \sum_{n \neq 0, n \in \mathbb{Z}_N^d} 1 = \frac{1}{4d\beta}(M-1)$$

which then implies the following upper bound for the individual local error at each site

$$\frac{V_c^{loc}}{M} \leq \frac{1}{4d\beta}.$$

Thus, the individual local error measure for the standard consensus algorithm is bounded from above for any network size in any dimension d.

The derivation of the macroscopic error upper bounds are a little more involved. First we observe that $V_c^{lrd} \leq 4V_c^{dav}$. This is easily seen since first, the sums in (27) and (28) involve terms that are all of the same sign (since $\hat{a}_n \leq 0$), and second, that the sum in (27) is taken over a subset of the terms in (28). It therefore suffices to derive the upper bounds for V_c^{dav}.

We begin with a simplifying observation. Because the arrays a we consider are real, their Fourier symbols $\hat{a}$ have even symmetry about all the mid axes of $\mathbb{Z}_N^d$. More precisely

$$\hat{a}_{(n_1,...,n_r,...,n_d)} = \hat{a}_{(n_1,...,N-n_r,...,n_d)}$$

for any of the dimension indices r. Assume for simplicity that N is odd, and define $\bar{N} := (N+1)/2$. The even symmetry property implies that the discrete hyper-cube $\mathbb{Z}_N^d$ can be divided into 2^d hyper-cubes, each of the size of $\mathbb{Z}_{\bar{N}}^d$, and over which the values of $\hat{a}$ can be generated from its values over $\mathbb{Z}_{\bar{N}}^d$ by appropriate reflections. Consequently, a sum like (28) can be reduced to

$$V_c^{dav} = -\frac{1}{2} \sum_{n \neq 0, n \in \mathbb{Z}_N^d} \frac{1}{\Re(\hat{a}_n)} = -\frac{2^d}{2} \sum_{n \neq 0, n \in \mathbb{Z}_{\bar{N}}^d} \frac{1}{\Re(\hat{a}_n)}.$$

We now calculate an upper bound on the deviation from average measure (28) for the Fourier symbol (32) of the standard consensus algorithm

$$\begin{aligned}
V_c^{dav} &= \frac{1}{4\beta} \sum_{n \neq 0, n \in \mathbb{Z}_N^d} \frac{1}{\sum_{r=1}^d \left(1 - \cos\left(\frac{2\pi}{N} n_r\right)\right)} \\
&= \frac{2^d}{4\beta} \sum_{n \neq 0, n \in \mathbb{Z}_{\bar{N}}^d} \frac{1}{\sum_{r=1}^d \left(1 - \cos\left(\frac{2\pi}{N} n_r\right)\right)} \\
&\leq \frac{2^d}{32\beta} N^2 \sum_{n \neq 0, n \in \mathbb{Z}_{\bar{N}}^d} \frac{1}{(n_1^2 + \cdots + n_d^2)} \quad (33)
\end{aligned}$$

where the first equality follows from reflection symmetry, and the inequality follows from (49), and noting that the denominator is made up of d terms of the form

$$1 - \cos\left(\frac{2\pi}{N} n_r\right) \geq \frac{2}{\pi^2}\left(\frac{2\pi}{N} n_r\right)^2 = \frac{8}{N^2} n_r^2$$

where the inequality is valid in the range $n_r \in [0, (\bar{N}-1)]$.

The asymptotics of sums in (33) are presented in Appendix B. Using those expressions, we calculate the individual deviation from average measure at each site

$$\begin{aligned}
\frac{V_c^{dav}}{N^d} &\leq \frac{2^d}{32\beta} N^{2-d} \sum_{n \neq 0, n \in \mathbb{Z}_{\bar{N}}^d} \frac{1}{(n_1^2 + \cdots + n_d^2)} \\
&\approx \frac{2^d}{32\beta} N^{2-d} \begin{cases} \frac{1}{d-2}(\bar{N}^{d-2} - 1) & d \neq 2 \\ \log(\bar{N}) & d = 2 \end{cases} \\
&\leq \mathcal{C}_d \frac{1}{\beta} \begin{cases} N & d = 1 \\ \log(N) & d = 2 \\ 1 & d \geq 3, \end{cases} \quad (34)
\end{aligned}$$

where we have used $\bar{N} \leq N$, and $\mathcal{C}_d$ is a constant that depends on the dimension d, but is independent of N or the algorithm parameter β. We note that the upper bounds have exactly the same form when written in terms of the network size $M = N^d$.

B. Upper Bounds for Vehicular Formations

To establish upper bounds in this case, we use a feedback control law which is similar to (8). This law can be most compactly written in operator notation as

$$u = T_o \tilde{x} + T_o \tilde{v} + g_o \tilde{x} + f_o \tilde{v}$$

where T_o is the operator of convolution with the array O defined in the consensus problem (2). Note that in the multi-dimensional case, all signals are d-vectors, and thus T_o above is our notation for a diagonal operator with T_o in each entry of the diagonal. The last two terms represent absolute position and velocity error feedbacks respectively. The first two terms represent a feedback where each vector component of u_k is formed by a law like (1) from the corresponding vector components of $\tilde{x}_k$ and $\tilde{v}_k$ and all $2d$ immediate neighbor sites in the lattice.

With the above feedback law, the closed loop system (7) has the following expressions for the Fourier symbols of G and F

$$\hat{g}_n = g_o + \hat{O}_n, \quad \hat{f}_n = f_o + \hat{O}_n \quad (35)$$

where $\hat{O}$ is the Fourier symbol (32). We impose the additional conditions that $g_o \leq 0$ and $f_o \leq 0$ since otherwise the closed loop system will have an increasing number of strictly unstable modes as N increases. When $g_o \neq 0$ (respectively, $f_o \neq 0$) we refer to that feedback as using absolute position (respectively, velocity) feedback. There are four possible combinations of such feedback scenarios.

We now use these expressions for the symbols $\hat{g}$ and $\hat{f}$ to calculate upper bounds on performance measures **(P1)**, **(P2)** and **(P3)** for all four feedback scenarios. We begin with the local error (29) which in this case is given by

$$V_v^{loc} = \frac{-1}{4\beta} \sum_{n \neq 0, n \in \mathbb{Z}_N^d} \frac{\hat{O}_n}{(g_o + \hat{O}_n)(f_o + \hat{O}_n)}. \quad (36)$$

In the case of relative position and velocity error feedback, which corresponds to $g_o = 0$ and $f_o = 0$, the sum in (36) becomes $-\sum 1/\hat{O}_n$. This has the same form as V_c^{dav} in (28) for the standard consensus problem, and thus will grow asymptotically as derived in (34). For this scenario, the final answer is listed as V_v^{loc} in Table I after multiplying by the extra $1/\beta$ factor. In the case of relative position and absolute

velocity feedback, the sum in (36) becomes $\sum -1/(f_o + \hat{O}_n)$. Each term is bounded from above by $-1/(f_o + \hat{O}_n) \leq -1/f_o$ since $f_o < 0$ and $\hat{O}_n \leq 0$. Thus the entire sum has an upper bound that scales like M, which yields a constant bound for the individual local error once divided by the network size M. An exactly symmetric argument applies to the case of absolute position but relative velocity feedback. Finally, in the case of both absolute position and velocity feedback $f_o < 0$ and $g_o < 0$ implying a uniform bound on each term in the sum. Similarly the entire sum scales like M and thus is uniformly bounded upon division by the network size. All of these four cases for the local error scalings are summarized in Table I.

We now consider the case of the deviation from average measure (31) which for our specific algorithm is

$$V_v^{dav} = \frac{d}{2} \sum_{n \neq 0, n \in \mathbb{Z}_N^d} \frac{1}{(g_o + \hat{O}_n)(f_o + \hat{O}_n)}.$$

When $g_o < 0$ and $f_o < 0$, each term in the sum is bounded and the entire sum scales as M. Thus, the individual deviation from average at each site is bounded in this case. When either $f_o = 0$ or $g_o = 0$, then the sums scale like $-\sum 1/\hat{O}_n$ (since the other factor in the fraction is uniformly bounded), i.e. like the deviation from average in the consensus case (34).

The only case that requires further examination is that of relative position and relative velocity feedback ($g_o = f_o = 0$). In this case

$$V_v^{dav} = \frac{d}{2} \sum_{n \neq 0, n \in \mathbb{Z}_N^d} \frac{1}{\hat{O}_n^2}$$

$$\leq \frac{d 2^d}{2^8} \frac{1}{\beta^2} N^4 \sum_{n \neq 0, n \in \mathbb{Z}_N^d} \frac{1}{(n_1^2 + \cdots + n_d^2)^2}$$

where the inequality is derived by the same argument used in deriving the inequality (33). Dividing this expression by the network size N^d and using the asymptotic expressions (52) yields

$$\frac{V_v^{dav}}{N^d} \leq \mathcal{C}_d \frac{1}{\beta^2} \begin{cases} \frac{1}{d-4}(1 - N^{4-d}) & d \neq 4 \\ \log(N) & d = 4, \end{cases} \quad (37)$$

where $\mathcal{C}_d$ is a constant depending on the dimension d but independent of N or the algorithm parameter β. Rewriting these bounds in terms of the total network size $M = N^d$ gives the corresponding entries in Table I, where the other cases are also summarized.

We finally point out that $V_v^{lrd} \leq 4 V_v^{dav}$ due to an argument identical to that employed in the consensus case. We thus conclude that the upper bounds just derived apply to the case of the long range deviation measure as well.

The Role of Viscous Friction: It is interesting to observe that in vehicular models with viscous friction (6), a certain amount of absolute velocity feedback is inherently present in the dynamics. The model (6) with a feedback control of the form (8) has the following Fourier symbol for the velocity feedback operator F

$$\hat{f}_n = -\mu + f_o + \hat{O}_n.$$

We conclude that even in cases of only relative velocity error feedback (i.e. when $f_o = 0$), the viscous friction term $\mu >$ 0 provides some amount of absolute velocity error feedback. Thus, in an environment which has viscous damping, performance in vehicle formation problems scale in a similar manner to consensus problems. These comments are also applicable to the lower bounds developed in the next section.

The Role of Control Effort: A common feature of all the asymptotic upper bounds of the standard algorithms just presented is their dependence on the parameter β. If this parameter is fixed in advance based on design considerations, then the algorithm's performance will scale as shown in Table I. However, it is possible to consider the redesign of the algorithms as the network size increases. For example, it is possible to increase β proportionally to M in consensus algorithms to achieve bounded macroscopic errors even for 1-D networks. As can be seen from (1), this has the effect of increasing the control feedback gains unboundedly (in M), which would clearly be unacceptable in any realistic control problem. Thus, any consideration of the fundamental limits of performance of more general algorithms must account for some notion of control effort, and we turn to this issue in the next section.

V. LOWER BOUNDS

A natural question arises as to whether one can design feedback controls with better asymptotic performance than the standard algorithms presented in the previous section. In this section we analyze the performance of any linear static state feedback control algorithm satisfying the structural assumptions **(A1)–(A5)**, and subject to a constraint on control effort. A standard measure of control effort in stochastic settings is the steady state variance of the control signal at each site

$$\mathcal{E}\{u_k^* u_k\} \quad (38)$$

which is independent of k due to the spatial invariance assumption. We constrain this quantity and derive lower bounds on the performance of any algorithm that respects this constraint. The basic conclusion is that lower bounds on performance scale like the upper bounds listed in Table I with the control effort replacing the parameter β. In other words, *any algorithm with control effort constraints will not do better asymptotically than the standard algorithms* of Section IV-B. This is somewhat surprising given the extra degrees of freedom possible through feedback control design, and it perhaps implies that it is primarily the network topology and the structural constraints, rather than the selection of the algorithm's parameters that determine these fundamental limitations.

We now turn to the calculation of lower bounds on both microscopic and macroscopic performance measures. For brevity, we include only the calculations for the deviation from average macroscopic measures. These calculations are a little more involved than those for the upper bounds since they need to be valid for an entire class of feedback gains. However, the basic ideas of utilizing H^2 norms are similar, and this is what we do in the sequel. In addition, a new ingredient appears where the control effort bound, combined with the locality property, implies a uniform bound on the entries of the feedback arrays. This is stated precisely in the next lemma whose proof is found in the Appendix. These bounds then finally impose lower bounds on the performance of control-constrained local algorithms.

Lemma 5.1: Consider general consensus (4) and vehicular formation (7) algorithms where the feedback arrays a, g and f posses the locality property (A3). The following bounds hold:

$$\|a\|_\infty \leq \mathcal{B}_a \mathcal{E}\{u_k^2\}$$
$$\|g\|_\infty \leq \mathcal{B}_g \left(\{\mathcal{E}u_k^2\}\right)^2$$
$$\|f\|_\infty \leq \mathcal{B}_f \mathcal{E}\{u_k^2\} \tag{39}$$

where $\mathcal{B}_a$, $\mathcal{B}_g$ and $\mathcal{B}_f$ are constants independent of the network size.

A. Lower Bounds for Consensus Algorithms

We start with the deviation from average measure for a stable consensus algorithm subject to a constraint of bounded control variance at each site

$$\mathcal{E}\{u_k^2\} \leq W. \tag{40}$$

We first observe a bound on $\Re(\hat{a}_n)$ that can be established from the definition of the Fourier transform

$$\Re(\hat{a}_n) = \Re\left(\sum_{k \in \mathbb{Z}_N^d} a_k e^{-i\frac{2\pi}{N}(n.k)}\right)$$
$$= \sum_{k \in \mathbb{Z}_N^d} a_k \cos\left(\frac{2\pi}{N}n \cdot k\right)$$
$$= \sum_{k \in \mathbb{Z}_N^d} a_k \left[1 - \left(1 - \cos\left(\frac{2\pi}{N}n \cdot k\right)\right)\right]$$
$$= \sum_{k \in \mathbb{Z}_N^d} (-a_k)\left(1 - \cos\left(\frac{2\pi}{N}n \cdot k\right)\right)$$

where the last equality is a consequence of the condition $\sum_{k \in \mathbb{Z}_N^d} a_k = 0$. For lower bounds on $\sum 1/\Re(-\hat{a}_n)$, upper bounds on $\Re(-\hat{a}_n)$ are needed. Observe that

$$|\Re(-\hat{a}_n)| = \left|\sum_{k \in \mathbb{Z}_N^d} a_k \left(1 - \cos\left(\frac{2\pi}{N}n \cdot k\right)\right)\right|$$
$$\leq \sum_{k \in \mathbb{Z}_N^d} |a_k|\left(1 - \cos\left(\frac{2\pi}{N}n \cdot k\right)\right)$$
$$\leq \frac{4\pi^2}{N^2} \sum_{k \in \mathbb{Z}_N^d} |a_k|(n \cdot k)^2$$

where the second inequality follows from (48). The last quantity can be further bounded by recalling the locality property (11), which has the consequence

$$\sum_{k \in \mathbb{Z}_N^d} |a_k|(k_1 n_1 + \cdots + k_d n_d)^2$$
$$= \sum_{k \in \mathbb{Z}_N^d, |k_i| \leq q} |a_k|(k_1 n_1 + \cdots + k_d n_d)^2$$
$$\leq \sum_{0 \neq k \in \mathbb{Z}_N^d, |k_i| \leq q} |a_k|(q n_1 + \cdots + q n_d)^2$$
$$= q^2 (n_1 + \cdots + n_d)^2 \sum_{0 \neq k \in \mathbb{Z}_N^d, |k_i| \leq q} |a_k|.$$

Now the locality property can be used again to bound the above sum using the the control effort bounds (39) and (40)

$$\sum_{0 \neq k \in \mathbb{Z}_N^d, |k_i| \leq q} |a_k| \leq (2q)^d \|a\|_\infty \leq (2q)^d \mathcal{B}_a W. \tag{41}$$

Putting the above together gives

$$V_c^{dav} = \sum_{n \neq 0, n \in \mathbb{Z}_N^d} \frac{1}{-\Re(\hat{a}_n)}$$
$$\geq \frac{N^2}{\pi^2 (2q)^{d+2} \mathcal{B}_a W} \sum_{n \neq 0, n \in \mathbb{Z}_N^d} \frac{1}{(n_1 + \cdots + n_d)^2}$$
$$\geq \frac{\mathcal{C}_d}{W} N^2 \sum_{n \neq 0, n \in \mathbb{Z}_N^d} \frac{1}{(n_1^2 + \cdots + n_d^2)}$$

where the last inequality follows from (50), and $\mathcal{C}_d$ is a constant independent of N.

Finally, utilizing (51) and dividing by the network size $M = N^d$, a lower bound on the deviation from average is obtained

$$\frac{V_c^{dav}}{N^d} \geq \frac{\mathcal{C}_d}{W} N^{2-d} \sum_{n \neq 0, n \in \mathbb{Z}_N^d} \frac{1}{(n_1^2 + \cdots + n_d^2)}$$
$$\approx \frac{\mathcal{C}_d}{W} \begin{cases} \frac{1}{d-2}(1 - N^{2-d}) & d \neq 2 \\ \log(N) & d = 2, \end{cases}$$
$$\geq \mathcal{C}_d \frac{1}{W} \begin{cases} N & d = 1 \\ \log(N) & d = 2 \\ 1 & d \geq 3, \end{cases} \tag{42}$$

where by a slight abuse of notation, we use $\mathcal{C}_d$ to denote different constants in the expressions above. We observe how the lower bounds (42) have the same asymptotic form as the upper bounds for the standard consensus algorithm (34), but with the control effort bound W replacing the parameter β.

B. Lower Bounds for Vehicular Formations

We recall the development of the upper bounds for vehicular formations in Section IV-B. The Fourier symbols of general feedback gains G and F have a similar form to (35), and as

$$\hat{g}_n = g_o + \hat{\gamma}_n, \quad \hat{f}_n = f_o + \hat{\phi}_n \tag{43}$$

where g_o, f_o and $\hat{\gamma}$, $\hat{\phi}$ are the absolute and relative feedback terms respectively. As before, we impose the conditions that $g_o, f_o \leq 0$. We assume that we have a control effort constraint of the form (40).

The case of absolute position and absolute velocity feedback has upper bounds which are finite, and the question of lower bounds is moot. For the other three cases, lower bounds on (31) are established using upper bounds on the symbols $\hat{g}$ and $\hat{f}$ which can be derived as follows:

$$\|\hat{f}\|_\infty \leq \|f\|_1 \leq (2q+1)\|f\|_\infty \leq (2q+1)\mathcal{B}_f W$$

where the inequalities follow from (46), the locality property, and (39), respectively. For g we similarly have

$$\|\hat{g}\|_\infty \leq (2q+1)\mathcal{B}_g W^2.$$

Consider now the case of relative position and absolute velocity feedback. A lower bound is established by

$$V_v^{dav} = \frac{d}{2} \sum_{n \neq 0, n \in \mathbb{Z}_N^d} \frac{1}{|\hat{g}_n||\hat{f}_n|}$$

$$\geq \frac{d}{2(2q+1)\mathcal{B}_f} \frac{1}{W} \sum_{n \neq 0, n \in \mathbb{Z}_N^d} \frac{1}{|\hat{g}_n|}.$$

Now a lower bound on the sum can be established in exactly the same manner as (42) in the consensus case since $\hat{g}$ is a symbol of a local relative feedback operator. The case of relative velocity and absolute position feedback is similar with the exception that the factor of $1/W$ is replaced by $1/W^2$.

The final case to consider is that of relative position and relative velocity feedback. One can repeat the same arguments made in the consensus case up to (41) for both $\hat{g}_n$ and $\hat{f}_n$ to state

$$\sum_{0 \neq n \in \mathbb{Z}_N^d} \frac{1}{|\hat{g}_n||\hat{f}_n|} \geq \frac{c_1 N^4}{\|g\|_\infty \|f\|_\infty} \sum_{0 \neq n \in \mathbb{Z}_N^d} \frac{1}{(n_1 + \cdots + n_d)^4}$$

$$\geq \frac{c_2 N^4}{W^3} \sum_{0 \neq n \in \mathbb{Z}_N^d} \frac{1}{(n_1 + \cdots + n_d)^4}$$

where c_1 and c_2 are some constants independent of N and W. The asymptotic behavior of this expression (divided by the network size) was given earlier in (37). We thus conclude that the lower bounds in this case are exactly like the upper bounds shown in Table I for relative position and relative velocity feedback, but with the $1/\beta^2$ term replaced by $1/W^3$.

VI. EXAMPLES AND MULTISCALE INTERPRETATION

Numerical simulations of cases where macroscopic measures grow unboundedly with network size show a particular type of motion for the entire formation. In the 1-D case, it can be described as an accordion-like motion in which large shape features in the formation fluctuate. Fig. 1 shows the results of a simulation of a 100 vehicle platoon with both relative position and relative velocity error feedbacks. This corresponds to a control strategy of the type for which upper bounds were calculated in Section IV-B with $g_o = f_o = 0$.

An interesting feature of these plots is the phenomenon of lack of formation coherence. This is only discernible when one "zooms out" to view the entire formation. The length of the formation fluctuates stochastically, but with a distinct slow temporal and long spatial wavelength signature. In contrast, the zoomed-in view in Fig. 1 shows a relatively well regulated vehicle-to-vehicle spacing. In general, it appears that small scale (both temporally and spatially) disturbances are well regulated, while large scale disturbances are not. An intuitive interpretation of this phenomenon is that local feedback strategies are unable to regulate against large scale disturbances.

In this paper, we have not directly analyzed the temporal and spatial scale dependent disturbance attenuation limits of performance. However, it appears that our microscopic and macroscopic measures of performance do indeed correspond to small and large scale (both spatially and temporally) motions respectively. We next outline a more mathematical argument that connects these measures.
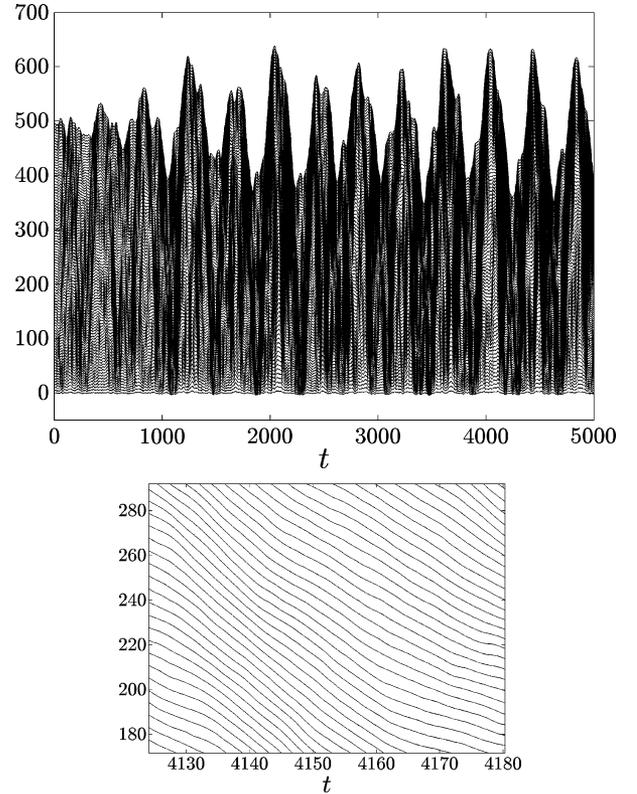

Fig. 1. Vehicle position trajectories (relative to vehicle number 1) of a 100 vehicle formation all of which are subjected to random disturbances. Top graph is a "zoomed out" view exhibiting the slow accordion-like motion of the entire formation. Bottom graph is a zoomed in view showing that vehicle-to-vehicle distances are relatively well regulated.

Mode Shapes: To appreciate the connection between H^2 norms and mode shapes in our system, consider first a general linear system driven by a white random process

$$\dot{x} = Ax + w.$$

When A is a normal matrix, it is easy to show (by diagonalizing the system with the orthonormal state transformation made up of the eigenvectors of A) that the steady state variance of the state is

$$\lim_{t \to \infty} \mathcal{E}\{x^*(t)x(t)\} = \sum_i \frac{1}{2\Re\{\lambda_i\}}$$

where the sum is taken over all the eigenvalues λ_i of A. Thus we can say that under white disturbance excitation, the amount of energy each mode contains is inversely proportional to its distance from the imaginary axis. In other words, slower modes are more energetic. Now, all the systems we consider in this paper are diagonalizable (or block-diagonlizable) by the spatial Discrete Fourier Transform. In addition, for the standard algorithms, we have the situation that *slow temporal modes correspond to long spatial wavelengths*. This provides an explanation for the observation that the most energetic motions are those that are temporally slow and have long spatial wavelengths.

String Instability: While string instability is sometimes an issue in formation control, the phenomenon we study in this paper is distinct from string instability. The example presented
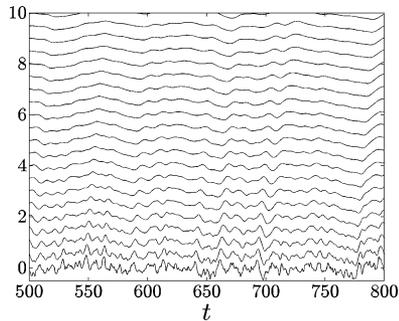
Fig. 2. Vehicle position trajectories (relative to leader) of the first few of a 100 vehicle formation. Only lead vehicle is subjected to random disturbances. Vehicle trajectories exhibit regulation against that disturbance, indicating the absence of string instability.

in this section is that of a formation that does posses string stability. For illustration, we repeat the simulation but with disturbances acting only on the first vehicle. The resulting vehicle trajectories are shown in Fig. 2. It is interesting to note that temporally high frequency disturbances appear to be very well regulated, and do not propagate far into the formation, while low temporal frequency disturbances appear to propagate deep into the formation. What is not shown in the figure is that low frequency disturbances are eventually regulated for vehicles far from the first. This is consistent with the intuitive notion discussed earlier that local feedback is relatively unable to regulate large scale disturbances.

Multi-Scale Properties of Disturbance Rejection: An intriguing explanation of the above example and our scaling results is as follows. The macroscopic error measures capture how well the network regulates against large-scale disturbances. In large, 1-D networks, local feedback alone is thus unable to regulate against these large-scale disturbances, and global feedback is required to achieve this. This seems rather intuitive. Perhaps surprisingly, in large networks with higher spatial dimensionality, local feedback alone can indeed regulate against large-scale disturbances. This follows for networks for which the macroscopic error measure is bounded irrespective of network size. The "critical dimension" needed to achieve this depends on the order of the node dynamics as well as the type of feedback strategy as shown in Table I (e.g. dimension 3 for relative position and absolute velocity feedback, and dimension 5 for relative position and velocity feedback in cases of vehicular formations).

VII. DISCUSSION

A. General Networks

The networks considered in this paper are ones which can be built on top of a Torus network. Some concepts, such as coherence and microscopic and macroscopic errors are easily generalized to arbitrary networks. The correct generalization of the concept of spatial dimension however is more subtle.

For any network of dynamical systems for which a distance metric is defined between nodes (e.g., from an imbedding of the network in $\mathbb{R}^n$), the notion of long range deviation can be defined as done in this paper. The calculation of that quantity involves system Grammians and may even be written in terms of the underlying system matrices for certain structures. Thus

coherence measures can be calculated numerically for such networks. However, more explicit calculations to uncover scaling laws as network size increases will clearly require more analytical expressions for the system norms in such networks.

To generalize the present results, one would require a notion of how to grow the network size while preserving certain topological properties such as the spatial dimension. Preliminary results on self-similar and fractal networks have been obtained [14]. The proper notion of spatial dimension to capture coherence in general graphs remains a research topic at this time.

B. Distributed Estimation and Resistive Lattices

The results presented here have a strong resemblance to results on performance limitations of distributed estimation algorithms based on network topology [15], [16], where asymptotic bounds similar to (34) first appeared in the controls literature (see also [17] where a consensus problem with noisy observations is analyzed yielding performance bounds like the consensus upper bounds we have in the present paper). In that work, the arguments are based on an analogy with effective resistance in resistive lattices and certain imbeddings of their graphs in d-dimensional space [18]. It is not clear how the resistive analogy can be generalized to cover the case of second order dynamics (i.e. vehicular formations), or the lower bounds on more general control laws. We have therefore avoided the resistive network analogy in this paper by directly using the multidimensional Fourier transform and reducing all calculations to sums of the form (51) resulting in a self-contained argument.

It is interesting to note that the original arguments for the asymptotic behavior in resistive lattices [19] in the physics literature are based on approximations of the Green's function of the diffusion operator in d-dimensions, for which the underlying techniques are approximations like (54).

C. Order of Local Dynamics

We have attempted to keep the development general enough that it is applicable to networked dynamical systems whose dynamics are not necessarily those of vehicles in any particular physical setting. What we refer to in this paper as consensus and vehicular formations problems respectively represent networks where the local dynamics (at each site) are first and second order chains of integrators respectively. The dynamical models are such that the stochastic disturbance enters into the first integrator, and the performance objectives involve variances of the outputs of the last integrators at each site. One generalization of this set up is where the local dynamics is a chain of n integrators. It is then possible to show that [by retracing the arguments for the vehicular formations case and generalizing (52)] the cutoff dimension to have bounded macroscopic measures with only local relative state feedback is $1 + 2n$.

D. LQR Designs

It was observed in [20] that optimal LQR designs for vehicular platoons suffer from a fundamental problem as the platoon size increases to infinity. These optimal feedback laws are almost local in a sense described by [21], where control gains decay exponentially as a function of distance. The resulting optimal feedbacks [20] suffer from the problem of having underdamped slow modes with long spatial wavelengths. Thus, the same incoherence phenomenon occurs in these optimal LQR

designs where the performance objective is composed of sums of local relative errors (leading to feedback laws with exponentially decaying gains on relative errors).

E. Measuring Performance in Large Scale Systems

In spatial dimensions where performance scalings are bounded, the underlying system eigenvalues still limit towards zero, suggesting ultimate instability in the limit as $M \to \infty$. However, measures of performance remain bounded in these cases. In such cases the locations of internal eigenvalues are not a good indication of the system's performance in the limit of large networks.

Take the consensus problem over $\mathbb{Z}_N^d$ as an example. The "least damped eigenvalue" (other than zero) quantifies the convergence time of deviation from average (in the absence of stochastic disturbances), and it scales as

$$\frac{1}{|\lambda_2|} = \Theta\left(N^{\frac{2}{d}}\right) \tag{44}$$

as can be shown by explicit eigenvalue calculations [12], [13]. If we use this quantity as a measure of performance, it indicates that performance becomes arbitrarily bad (in the limit of large N) in any spatial dimension d. On the other hand, consider the use of a macroscopic error measure like the variance of the deviation from average (19) in the presence of stochastic disturbances. That quantity can be expressed in terms of the system eigenvalues as

$$V_c^{dav} = \frac{1}{2N^d} \sum_{n \neq 0} \frac{1}{|\lambda_n|} \tag{45}$$

where the sum is taken over all the system's eigenvalues other than zero. Note that this sum is just (28) rewritten to emphasize the contrast with (44).

The important observation is that (44) indicates that as network size increases, the system eigenvalues approach the stability boundary, indicating an eventual catastrophic loss of performance in any spatial dimension d. On the other hand, (45) is uniformly bounded in dimensions $d \geq 3$ (as shown in (34)), thus implying well behaved systems as quantified by the macroscopic performance measures. A similar point to the above has been recently made [22].

The least damped eigenvalue is traditionally used as an important measure of performance. The examples in this paper demonstrate that for large scale systems, it is not a very meaningful measure of performance, and that the general question of how to measure performance in large scale systems is a subtle one.

F. Detuning/Mistuning Designs

It is shown in [23] that spatially-invariant local controllers for platoons have closed loop eigenvalues that approach the origin at a rate of $O(1/N^2)$. A "mistuning" design modification is proposed [23], resulting in spatially-varying local controllers where the closed loop eigenvalues approach the origin at the better rate of $O(1/N)$. In this paper, we have not used the real part of the least damped eigenvalue as a measure of performance but rather the variance of certain system outputs. This amounts

to using an H^2 norm as the measure of performance. It was shown in [21] that for spatially-invariant plants, one can not improve H^2 performance with spatially-varying controllers. The resulting controllers however have exponentially decaying gains rather than completely local gains. The problem of designing optimal H^2 controllers with a prescribed neighborhood of interaction remains an open and non-convex one. It is an interesting and open question as to whether mistuning designs for the H^2 measures we use in this paper can yield local controllers with better asymptotic performance than spatially-invariant ones. It was also shown [23] that a mistuning design can improve H^∞ performance for platoon problems. This shows that there is perhaps an important distinction between H^∞ and H^2 measures of performance for large scale systems. A point that is worthy of further investigation.

APPENDIX

A. Multidimensional Discrete Fourier Transform

We define the Discrete Fourier Transform for functions $\{f_k\}$ over $\mathbb{Z}_N^d$ by

$$\hat{f}_n := \sum_{k \in \mathbb{Z}_N^d} f_k e^{-i\left(\frac{2\pi}{N} n \cdot k\right)}$$

where $n \cdot k := n_1 k_1 + \cdots + n_d k_d$. The inverse transform is given by

$$f_k := \frac{1}{M} \sum_{n \in \mathbb{Z}_N^d} \hat{f}_k e^{i\left(\frac{2\pi}{N} n \cdot k\right)}$$

where $M = N^d$. An immediate consequence of the definitions are the following bounds:

$$\|\hat{f}\|_\infty \leq \|f\|_1, \quad \|f\|_\infty \leq \frac{1}{M}\|\hat{f}\|_1. \tag{46}$$

Let δ be the Kronecker delta on $\mathbb{Z}_N^d$. It's transform is the array $\mathbf{1}$, which is the array of all elements equal to 1. The transform of $\mathbf{1}$ is $M\delta$. We use the symbol $\bar{\mathbf{1}}$ to denote the array of all elements equal to $1/M$.

If T_f denotes the circulant operator of circular convolution with f, then the eigenvalues of T_f are just the numbers $\{\hat{f}_n\}$, and consequently the trace of T_f is given by the sum

$$\operatorname{tr}(T_f) = \sum_{n \in \mathbb{Z}_N^d} \hat{f}_n. \tag{47}$$

B. Bounds and Asymptotics of Sums

The following facts are useful in establishing asymptotic bounds.

1) For any $x \in \mathbb{R}$ and any $y \in [-\pi, \pi]$

$$1 - \cos(x) \leq x^2 \tag{48}$$

$$1 - \cos(y) \geq \frac{2}{\pi^2} y^2. \tag{49}$$

2) Given d integers $n_1, \ldots, n_d$

$$(n_1 + \cdots + n_d)^2 \leq (2d+1)\left(n_1^2 + \cdots + n_d^2\right). \tag{50}$$

Proof:

$$\left(\sum_i n_i\right)^2 = \sum_i n_i^2 + \sum_i \sum_{j\neq i} n_i n_j.$$

Using $n_i n_j \leq (\max\{n_i, n_j\})^2 \leq n_i^2 + n_j^2$, we get the bound

$$\left(\sum_i n_i\right)^2 \leq \sum_i n_i^2 + \sum_{i=1}^d \sum_{j\neq i} \left(n_i^2 + n_j^2\right)$$
$$\leq \sum_i n_i^2 + 2d \sum_i n_i^2.$$

3) In the limit of large N,

$$\sum_{\substack{n\neq 0 \\ n\in\mathbb{Z}_N^d}} \frac{1}{(n_1^2 + \cdots + n_d^2)} \approx \begin{cases} \frac{1}{d-2}(N^{d-2} - 1) & d \neq 2 \\ \log(N) & d = 2 \end{cases} \quad (51)$$

$$\sum_{\substack{n\neq 0 \\ n\in\mathbb{Z}_N^d}} \frac{1}{(n_1^2 + \cdots + n_d^2)^2} \approx \begin{cases} \frac{1}{d-4}(N^{d-4} - 1) & d \neq 4 \\ \log(N) & d = 4. \end{cases} \quad (52)$$

$$(53)$$

where $f(N) \approx g(N)$ is notation for

$$\underline{c}\, g(N) \leq f(N) \leq \overline{c}\, g(N)$$

for some constants $\overline{c}$ and $\underline{c}$ and all $N \geq \overline{N}$ for some $\overline{N}$.

Proof: We begin with (51). Upper and lower bounds on this sum can be derived by viewing it as upper and lower Rieman sums for the integral

$$\int \cdots \int \frac{1}{x_1^2 + \cdots + x_d^2} dx_1 \cdots dx_d$$

over the region $\Delta \leq r \leq 1$ for the lower bound, and $\Delta \leq r \leq \sqrt{d}$ for the upper bound. Here $\Delta = 1/N$, and the asymptotic behavior is determined by the lower limit on the integrals, so both upper and lower bounds behave the same asymptotically.

Using the grid points $x_1 = n_1\Delta, \ldots, x_d = n_d\Delta$, and using the volume increment Δ^d, we get

$$\int \cdots \int \frac{1}{x_1^2 + \cdots + x_d^2} dx_1 \cdots dx_d$$
$$\approx \Delta^d \sum_{n\neq 0, n\in\mathbb{Z}_N^d} \frac{1}{((\Delta n_1)^2 + \cdots + (\Delta n_d)^2)}$$
$$= \Delta^{d-2} \sum_{n\neq 0, n\in\mathbb{Z}_N^d} \frac{1}{(n_1^2 + \cdots + n_d^2)}. \quad (54)$$

Now the integral can be evaluated using hyperspherical coordinates by

$$\int \frac{1}{x_1^2 + \cdots + x_d^2} dx_1 \cdots dx_d$$
$$= \int_\Delta^1 \int_0^\pi \cdots \int_0^{2\pi} \frac{1}{r^2} r^{d-1} \sin^{d-2}(\phi_1) \ldots \sin(\phi_{d-2}) dr\, d\phi_1 \ldots$$
$$\times d\phi_{d-1}$$
$$= C_d \int_\Delta^1 r^{d-3} dr$$

where C_d is a constant that depends only on the dimension d (and can be expressed in terms of the volume of the unit sphere in $\mathbb{R}^d$). Evaluating this integral, using $\Delta = 1/N$ and (54) gives the result (51).

The proof of (52) is very similar to the above, with the exception that one approximates the integral of $1/(x_1^2 + \cdots + x_d^2)^2 = 1/r^4$ instead. The details are omitted for brevity.

C. Proof of Lemma 3.1

For the consensus problem, the state equation is (4), and thus the Lyapunov (23) becomes

$$\hat{a}_n^* \hat{p}_n + \hat{p}_n \hat{a}_n = -\hat{\mathbb{C}}_n^* \hat{\mathbb{C}}_n$$

where we have used $H = C$ (and the choice of C depends on the particular performance measure being considered). Since all quantities are scalars, this equation is immediately solved for $\hat{p}_n = -\hat{\mathbb{C}}_n^* \hat{\mathbb{C}}_n / 2\Re(\hat{a}_n)$ for $n \neq 0$. In the case $n = 0$, we look at the integral definition (22), conclude that $\hat{\mathbb{C}}_0 = 0$ implies that $\hat{p}_0 = 0$. Thus, the sum (21) is calculated to be (24).

For the vehicular problem, the state equation is (7) with the output equation $H = [C\ 0]$. The Lyapunov (23) becomes

$$\begin{bmatrix} 0 & \hat{G}_n^* \\ I & \hat{F}_n^* \end{bmatrix} \begin{bmatrix} \hat{X}_n & \hat{Z}_n \\ \hat{Z}_n^* & \hat{Y}_n \end{bmatrix} + \begin{bmatrix} \hat{X}_n & \hat{Z}_n \\ \hat{Z}_n^* & \hat{Y}_n \end{bmatrix} \begin{bmatrix} 0 & I \\ \hat{G}_n & \hat{F}_n \end{bmatrix} = \begin{bmatrix} -\hat{\mathbb{C}}_n^* \hat{\mathbb{C}}_n & 0 \\ 0 & 0 \end{bmatrix}$$

where each of the submatrices is of size $d \times d$. From the above, we extract the following matrix equations:

$$\hat{G}_n^* \hat{Z}_n^* + \hat{Z}_n \hat{G}_n = -\hat{\mathbb{C}}_n^* \hat{\mathbb{C}}_n \quad (55)$$
$$\hat{G}_n^* \hat{Y}_n + \hat{X}_n + \hat{Z}_n \hat{F}_n = 0$$
$$\hat{Z}_n + \hat{F}_n^* \hat{Y}_n + \hat{Z}_n^* + \hat{Y}_n \hat{F}_n = 0. \quad (56)$$

Since we are only interested in the quantity

$$\operatorname{tr}\left(\hat{B}_n^* \hat{P}_n \hat{B}_n\right) = [0\ \ I] \begin{bmatrix} \hat{X}_n & \hat{Z}_n \\ \hat{Z}_n^* & \hat{Y}_n \end{bmatrix} \begin{bmatrix} 0 \\ I \end{bmatrix} = \operatorname{tr}(\hat{Y}_n)$$

then only (55) and (56) are relevant. The coordinate decoupling assumption (A5) on the operators G, F and C implies that the matrices $\hat{G}_n$, $\hat{F}_n$ and $\hat{\mathbb{C}}_n$ are all diagonal. It follows that $\hat{Z}_n$, $\hat{X}_n$ and $\hat{Y}_n$ are also diagonal, and the above matrix equations are trivial to solve. $\hat{Z}_n$ has the solution:

$$Z = -\frac{1}{2} \hat{G}_n^{-1} \hat{\mathbb{C}}_n^* \hat{\mathbb{C}}_n.$$

Similarly, (56) is solved to yield

$$Y = \frac{1}{2} (\hat{G}_n \hat{F}_n)^{-1} \hat{\mathbb{C}}_n^* \hat{\mathbb{C}}_n$$

for $n \neq 0$. For the unstable mode at $n = 0$, the integral (22) can be easily evaluated to yield $\hat{Z}_0 = 0$ (since $\hat{\mathbb{C}}_0 = 0$ for all the performance measures we consider). Adding in the assumption that all matrices are diagonal with equal elements, we obtain in summary the total H^2 norm of the vehicle formation problem (7) is given by

$$V_v = \frac{d}{2} \sum_{n\neq 0} \sum_{n\in\mathbb{Z}_N^d} \frac{\hat{c}_n^* \hat{c}_n}{\hat{g}_n \hat{f}_n} \quad (57)$$

where the multiplicative factor of d comes from taking the trace of $\hat{Y}_n$.

Proof of Corollary 3.2:

1) Consensus: The local error measure output operator C is given by (15), for which $C^*C = (-1/2d\beta)O$ by the identity (16). Combining this with Lemma 3.1 gives the result for V_c^{loc}.

The long range deviation measure has the output operator defined in (18), which has the Fourier symbol

$$\hat{c}_n = 1 - e^{-i\pi(n_1 + \cdots + n_d)}$$

from which we conclude that

$$\hat{c}_n = \begin{cases} 0 & (n_1 + \cdots + n_d) \text{ even} \\ 2 & (n_1 + \cdots + n_d) \text{ odd.} \end{cases}$$

Combining this with Lemma 3.1 gives the result for V_c^{lrd}.

The deviation from average output operator is $C = I - T_1$, or equivalently, the convolution operator $T_{\delta^0 - 1}$. The corresponding Fourier symbol is the Fourier transform of the array $\delta^0 - 1$, which gives

$$\hat{c}_n = 1_n \delta_n = \begin{cases} 0 & n = 0 \\ 1 & n \neq 0. \end{cases}$$

Putting this in the general formula (24) yields the result for V_c^{dav}.

2) Vehicular Formations: The derivations for this case are very similar to those for the consensus problem and are therefore omitted for brevity.

Proof of Lemma 5.1: We rewrite the dynamics of the consensus algorithm so that u is an output

$$\ddot{x} = T_a x = w$$
$$u = T_a x.$$

The present task is then to calculate the H^2 norm from w to u. Applying formula (24) with T_a as the C operator yields

$$\sum_{k \in \mathbb{Z}_N^d} \varepsilon\{u_k^2\} = \frac{-1}{2} \sum_{n \neq 0, n \in \mathbb{Z}_N^d} \frac{\hat{a}_n^2}{\hat{a}_n} = \frac{1}{2} \sum_{n \in \mathbb{Z}_N^d} (-\hat{a}_n)$$

after observing that $\hat{a}_n$ is real and $\hat{a}_0 = 0$. Furthermore, our stability condition requires that for all n, $(-\hat{a}_n) \geq 0$, implying that the sum above is the ℓ^1-norm of $\{\hat{a}_n\}$. Putting this together with the bound (46) gives

$$\|a\|_\infty \leq \frac{1}{M}\|\hat{a}\|_1 = 2\varepsilon\{u_k^2\}. \tag{58}$$

In the vehicular formations case, the dynamics are given by (7) together with the output equation

$$u = \begin{bmatrix} G & F \end{bmatrix} \begin{bmatrix} \tilde{x} \\ \tilde{v} \end{bmatrix}.$$

Formula (25) is not applicable here since the output depends on all states, but the H^2 norm for this system can be calculated in a manner similar to the proof of Lemma 3.1. They Lyapunov equation in this case becomes

$$\begin{bmatrix} 0 & \hat{G}_n^* \\ I & \hat{F}_n^* \end{bmatrix} \begin{bmatrix} \hat{X}_n & \hat{Z}_n \\ \hat{Z}_n^* & \hat{Y}_n \end{bmatrix} + \begin{bmatrix} \hat{X}_n & \hat{Z}_n \\ \hat{Z}_n^* & \hat{Y}_n \end{bmatrix} \begin{bmatrix} 0 & I \\ \hat{G}_n & \hat{F}_n \end{bmatrix}$$
$$= -\begin{bmatrix} -\hat{G}_n^*\hat{G}_n & \hat{G}_n^*\hat{F}_n \\ \hat{F}_n^*\hat{G}_n & \hat{F}_n^*\hat{F}_n \end{bmatrix}$$

from which we extract the matrix equations

$$\hat{G}_n^*\hat{Z}_n^* + \hat{Z}_n\hat{G}_n = -\hat{G}_n^*\hat{G}_n$$
$$\hat{G}_n^*\hat{Y}_n + \hat{X}_n + \hat{Z}_n\hat{F}_n = -\hat{G}_n^*\hat{F}_n$$
$$\hat{Z}_n + \hat{F}_n^*\hat{Y}_n + \hat{Z}_n^* + \hat{Y}_n\hat{F}_n = -\hat{F}_n^*\hat{F}_n.$$

Only the first and last equation need be solved since we are only interested in $\text{tr}(\hat{Y}_n)$. All of the above are $d \times d$ diagonal matrices with equal entries, so we solve the equations in terms of a single entry as

$$2\hat{g}_n\hat{z}_n = -\hat{g}_n^2 \Rightarrow \hat{z}_n = -\frac{1}{2}\hat{g}$$
$$2\hat{f}_n\hat{y}_n = -\hat{f}_n^2 - 2\hat{z}_n \Rightarrow \hat{y}_n = \frac{1}{2}(-\hat{f}_n + \frac{1}{\hat{f}_n}\hat{g}_n)$$

The H^2 norm of the system is then

$$\sum_{0 \neq n \in \mathbb{Z}_N^d} tr(\hat{Y}_n) = \frac{d}{2} \sum_{0 \neq n \in \mathbb{Z}_N^d} (-\hat{f}_n + \frac{1}{\hat{f}_n}\hat{g}_n)$$
$$= \frac{d}{2}(\|\hat{f}\|_1 + \|\frac{1}{\hat{f}}\hat{g}_n)$$

where the last equation follows from the stability conditions $\hat{f}_n \leq 0$, $\hat{g}_n \leq 0$. This inequality has two consequences after observing that $\sum_{n \in \mathbb{Z}_N^d} \text{tr}(\hat{Y}_n) = M\mathcal{E}\{u_k^2\}$ and using (46)

$$\|f\|_\infty \leq \frac{2}{d}\varepsilon\{u_k^2\} \tag{59}$$
$$\|\frac{1}{\hat{f}}\hat{g}\|_1 \leq \frac{2}{d}M\varepsilon\{u_k^2\}. \tag{60}$$

The second inequality can be used to bound $\|g\|_\infty$ as follows. First

$$\|\frac{1}{\hat{f}}\hat{g}\|_1 \geq \|\hat{g}\|_1 \min_n |\frac{1}{\hat{f}_n}| = \|\hat{g}\|_1 \frac{1}{\|\hat{f}\|_\infty}$$

An upper bound on $\|\hat{f}\|_\infty$ is derived from

$$\|\hat{f}\|_\infty \leq \|\hat{f}\|_1 \leq (2q)^d\|f\|_\infty$$

where the last inequality follows from the locality assumption on f. Combining these last two bounds with (60) yields

$$\frac{2}{d}M\varepsilon\{u_k^2\} \geq \frac{1}{(2q)^d\|f\|_\infty}\|g\|_1 \geq \frac{1}{(2q)^d\|f\|_\infty}M\|g\|_\infty$$

which when combined with (59) gives

$$\|g\|_\infty \leq \frac{2(2q)^d}{d}\|f\|_\infty\varepsilon\{u_k^2\} \leq B_g\left(\varepsilon\{u_k^2\}\right)^2.$$

REFERENCES

[1] S. Shladover, C. Desoer, J. Hedrick, M. Tomizuka, J. Walrand, W.-B. Zhang, D. McMahon, H. Peng, S. Sheikholeslam, and N. McKeown, "Automated vehicle control developments in the path program," *IEEE Trans. Veh. Technol.*, vol. 40, no. 1, pp. 114–130, Feb. 1991.

[2] D. Swaroop and J. K. Hedrick, "Constant spacing strategies for platooning in automated highway systems," *Trans. ASME J. Dyn. Syst., Meas. Control*, vol. 121, no. 3, pp. 462–470, Sep. 1999.

[3] D. Swaroop and J. K. Hedrick, "String stability of interconnected systems," *IEEE Trans. Autom. Control*, vol. 41, no. 2, pp. 349–357, Mar. 1996.

[4] S. M. Melzer and B. C. Kuo, "Optimal regulation of systems described by a countably infinite number of objects," *Automatica*, vol. 7, no. 3, pp. 359–366, May 1971.

[5] W. S. Levine and M. Athans, "On the optimal error regulation of a string of moving vehicles," *IEEE Trans. Autom. Control*, vol. AC-11, no. 3, pp. 355–361, Jul. 1966.

[6] S. Martinez, J. Cortes, and F. Bullo, "Motion coordination with distributed information," *Control Syst. Mag.*, vol. 27, no. 4, pp. 75–88, 2007.

[7] L. Xiao, S. Boyd, and S.-J. Kim, "Distributed average consensus with least-mean-square deviation," *J. Parallel Distrib. Comp.*, vol. 67, pp. 33–46, 2007.

[8] S. Patterson, B. Bamieh, and A. El Abbadi, "Distributed average consensus with stochastic communication failures," in *Proc. 46th IEEE Conf. Decision Control*, 2007, pp. 4215–4220.

[9] J. N. Tsitsiklis, "Problems in Decentralized Decision Making and Computation," Ph.D. dissertation, MIT, Cambridge, MA, 1985.

[10] J. E. Boillat, "Load balancing and poisson equation in a graph," *Concurrency: Practice and Experience*, vol. 2, no. 4, pp. 289–313, 1990.

[11] A. Jadbabaie, J. Lin, and A. S. Morse, "Coordination of groups of mobile autonomous agnets using neaqrst neighbor rules," *IEEE Trans. Autom. Control*, vol. 48, no. 6, pp. 988–1001, Jun. 2003.

[12] S. Patterson, B. Bamieh, and A. El Abbadi, "Brief announcement: Convergence analysis of scalable gossip protocols," in *Proc. 20th Int. Symp. Distrib. Comp.*, 2006, pp. 540–542.

[13] R. Carli, F. Fagnani, A. Speranzon, and S. Zampieri, "Communication constraints in the average consensus problem," *Automatica*, vol. 44, no. 3, pp. 671–684, 2007.

[14] S. Patterson and B. Bamieh, "Network coherence in fractal graphs," in *Proc. IEEE Conf. Decision Control (CDC)*, Dec. 2011, pp. 6445–6450.

[15] P. Barooah and J. P. Hespanha, "Estimation on graphs from relative measurements: Distributed algorithms and fundamental limits," *IEEE Control Syst. Mag.*, vol. 27, no. 4, pp. 57–74, 2007.

[16] P. Barooah and J. P. Hespanha, "Estimation from relative measurements: Electrical analogy and large graphs," *IEEE Trans. Signal Processing*, vol. 56, no. 6, pp. 2181–2193, Jun. 2008.

[17] P. Barooah and J. P. Hespanha, "Graph effective resistance and distributed control: Spectral properties and applications," in *Proc. IEEE Conf. Decision Control*, 2006, pp. 3479–3485.

[18] P. Doyle and J. Snell, "Random walks and electric networks, ser," in *The Carus Mathematical Monographs*. Washington, DC: The Mathematical Association of America, 1984.

[19] J. Cserti, "Application of the lattice Green's function for calculating the resistance of an infinite network of resistors," *Amer. J. Phys.*, vol. 68, p. 896, 2000.

[20] M. Jovanovic and B. Bamieh, "On the ill-posedness of certain vehicular platoon control problems," *IEEE Trans. Autom. Control*, vol. 50, no. 9, pp. 1307–1321, Sep. 2005.

[21] B. Bamieh, F. Paganini, and M. A. Dahleh, "Distributed control of spatially-invariant systems," *IEEE Trans. Autom. Control*, vol. 47, no. 7, pp. 1091–1107, Jul. 2002.

[22] R. Carli, F. Garin, and S. Zampieri, "Quadratic indicies for the analysis of consensus algorithms," in *Proc. Inform. Theory Appl. Workshop*, 2009 [Online]. Available: http://ita.ucsd.edu/workshop/09/talks/

[23] P. Barooah, P. G. Mehta, and J. P. Hespanha, "Mistuning-based decentralized control of vehicular platoons for improved closed loop stability," *IEEE Trans. Autom. Control*, vol. 54, no. 9, pp. 2100–2113, Sep. 2009.

Bassam Bamieh (M'90–SM'02–F'08) received the B.S. degree in electrical engineering and physics from Valparaiso University, Valparaiso, IN, in 1983, and the M.Sc. and Ph.D. degrees from Rice University, Houston, TX, in 1986 and 1992 respectively.

From 1991 to 1998 he was with the Department of Electrical and Computer Engineering and the Coordinated Science Laboratory, University of Illinois at Urbana-Champaign. He is currently a Professor of mechanical engineering at the University of California at Santa Barbara. His current research interests are in distributed systems, shear flow turbulence modeling and control, and thermo-acoustic energy conversion devices.

Dr. Bamieha received the AACC Hugo Schuck Best Paper Award, the IEEE CSS Axelby Outstanding Paper Award, and an NSF CAREER Award. He is a Fellow of IFAC and a Control Systems Society Distinguished Lecturer.

Mihailo R. Jovanović (S'00–M'05) received the Dipl. Ing. and M.S. degrees from the University of Belgrade, Belgrade, Serbia, in 1995 and 1998, respectively, and the Ph.D. degree from the University of California, Santa Barbara, in 2004.

Before joining the University of Minnesota, Minneapolis, he was a Visiting Researcher with the Department of Mechanics, the Royal Institute of Technology, Stockholm, Sweden, from September to December 2004. Currently, he is an Associate Professor of electrical and computer engineering at the University of Minnesota, where he serves as the Director of Graduate Studies in the interdisciplinary Ph.D. program in Control Science and Dynamical Systems. His expertise is in modeling, dynamics, and control of large-scale and distributed systems and his current research focuses on sparsity-promoting optimal control, dynamics and control of fluid flows, and fundamental limitations in the control of vehicular formations.

Dr. Jovanović received the CAREER Award from the National Science Foundation in 2007, and the Early Career Award from the University of Minnesota Initiative for Renewable Energy and the Environment in 2010. He is a member of APS and SIAM and has served as an Associate Editor of the IEEE Control Systems Society Conference Editorial Board from July 2006 until December 2010.

Partha Mitra (M'05–SM'12) received the Ph.D. degree in theoretical physics from Harvard University, Cambridge, MA, in 1993.

He worked in quantitative neuroscience and theoretical engineering at Bell Laboratories, Murray Hill, NJ, from 1993 to 2003, and as an Assistant Professor in theoretical physics at Caltech, Pasadena, CA, in 1996, before moving to Cold Spring Harbor Laboratory, Cold Spring Harbor, NY, in 2003, where he is currently Crick-Clay Professor of Biomathematics. Currently, he is leading the Mouse Brain Architecture Project to generate a brain-wide map of neuronal circuits in mouse. His research interests span multiple models and scales, combining experimental, theoretical and informatics approaches toward achieving an integrative understanding of complex biological systems, and of neural systems in particular.

Stacy Patterson (A'10) received the B.A. degree in mathematics and the B.S. degree in computer science from Rutgers University, Piscataway, NJ, in 1998, and the M.S. and Ph.D. degrees in computer science from the University of California at Santa Barbara, in 2003 and 2009, respectively.

From July 2009 to August 2011, she was a Postdoctoral Scholar at the Center for Control, Dynamical Systems, and Computation, University of California, Santa Barbara. She is currently a Postdoctoral Fellow in the Department of Electrical Engineering, Technion Israel Institute of Technology, Haifa, Israel. Her research interests include distributed systems, vehicle networks, and cloud computing.